THE JOURNAL OF PHYSICAL CHEMISTRY C

Article

pubs.acs.org/JPCC

Electronic and Field Emission Properties of Wrinkled Graphene

Yufeng Guo* and Wanlin Guo

State Key Laboratory of Mechanics and Control of Mechanical Structures and MOE Key Laboratory for Intelligent Nano Materials and Devices, Institute of Nanoscience, Nanjing University of Aeronautics and Astronautics, Nanjing 210016, China

ABSTRACT: Wrinkles can be seen as a kind of protrusion formed on the surface of graphene sheets. The response of the electronic properties of graphene wrinkles to charge injecting and external electric field, which is closely related to field emission properties, has been extensively studied by our first-principles calculations. We find that increasing the wrinkle size and its top curvature not only improves the field enhancement factor of the wrinkled graphene but also decreases the electron affinities and ionization potentials. When injecting charges, both the charge accumulation and depletion mostly distribute at the top parts of the wrinkles and become more concentrated in the wrinkle with a higher curvature. The change of the highest occupied molecular orbital and the lowest unoccupied molecular orbital caused by electric field mainly locates at the wrinkled parts, especially at its top. These results demonstrate that wrinkled graphene could be a good candidate for field emitter.

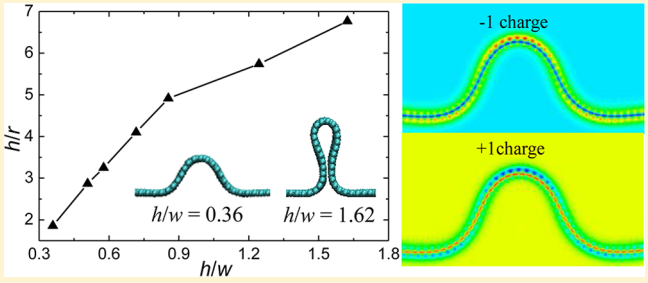

1. INTRODUCTION

Graphene, one of the thinnest two-dimensional materials, has exceptional mechanical[1−3] and physical properties[4−6] and is expected to be widely used in high performance functional devices. Because of high aspect ratio, excellent thermal stability, and electric conductivity, graphene and its derivatives are also attractive for field emission applications. A number of studies have reported that graphene composite films,[7−10] graphene oxide,[11] single-layer graphene sheets,[12] and graphene nanoribbons[13] in the presence of electric fields exhibit good field emission properties with low threshold field, high emission density, and good emission stability. The edges of graphene sheets are usually considered to play a key issue for emitting electrons and improving field-enhancement factor.[7,11,12] Nevertheless, to align graphene edges along a desired direction under applied electric field for field emission remains a great technical challenge. A recently experiment demonstrates highly efficient electron field emission from graphene oxide sheets, which is dramatically enhanced by a high density of sharp graphene protrusions formed on nickel nanotip arrays.[14] Similar field emission has also been observed for highly wrinkled hydrogen exfoliated graphene.[10] However, the underlying mechanism for the protrusions improving electron emission and the effects of surface morphology and structural deformation of graphene on its field emission properties are still unclear.

On the other hand, graphene can easily wrinkle on substrates into disordered states due to the compressive effect from substrates and low bending rigidity of graphene.[15−18] The geometry, amplitude, and size of graphene wrinkles now can be effectively manipulated and controlled by a lot of mechanical and thermal methods, such as cooperating with substrate morphology,[19] using the atomic force microscopy tips,[20] and thermally induced compression.[21,22] Wrinkled graphene leads to new physical phenomena and is playing an increasingly important role in designing novel nanoelectromechanical systems and patterning graphene nanostructures.[23−25] Graphene wrinkles can be considered as a kind of protrusion formed on the surface of graphene sheets. Further study on electronic properties and field emission mechanism of wrinkled graphene will be helpful for understanding the structural influence on graphene field emitters and the development of graphene-based electronic devices.

In this study, we have studied the electronic properties of wrinkled graphene and its response to charge injecting and external electric field by first-principles calculations. Wrinkled graphene is semiconducting, but its energy gap decreases with enlarging wrinkle size. The field enhancement factor of the wrinkled graphene increases with increasing wrinkle top curvature. The wrinkles slightly influence the work functions but reduce the electron affinities and ionization potentials of the wrinkled-graphene sheets. When injecting one negative and one positive charge, both the charge accumulation and depletion mostly locate at the top parts of the wrinkles. In the presence of electric fields, the work function of highly wrinkled graphene decreases quickly, and the charge distributions of the highest occupied molecular orbital (HOMO) and the lowest unoccupied molecular orbital (LUMO) as well as the local density of states are significantly modified at the wrinkled parts. All these results demonstrate that the wrinkles in graphene could be ideal field-emission electron sources.

Received: October 17, 2012
Revised: December 13, 2012
Published: December 17, 2012

   dx.doi.org/10.1021/jp3103063 | J. Phys. Chem. C 2013, 117, 692−696

2. MODEL AND METHOD

To obtain wrinkled graphene, we first perform molecular dynamics (MD) simulations in a NVT ensemble at 300 K by a Nose−Hoover thermostat, which are implemented in the LAMMPS package.[26] As shown in Figure 1a, the wrinkles are

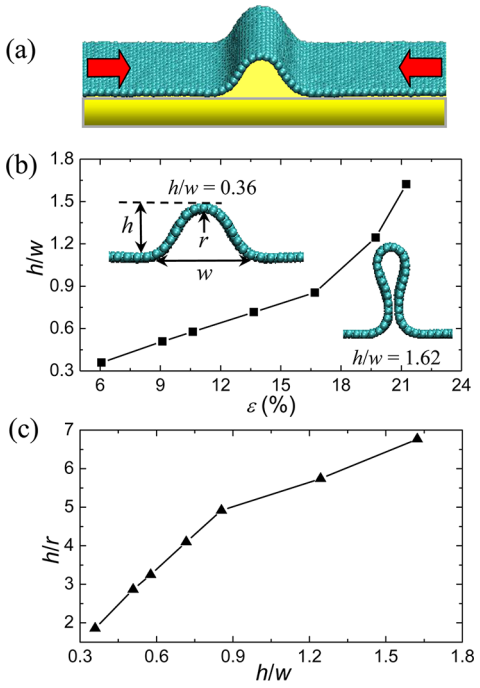

Figure 1. (a) A wrinkle is created by applying a uniaxial in-plane compression on substrate-supported graphene sheet. The variations of (b) the size ratio h/w of wrinkle height to width with the compressive strain ε and (c) the h/r of height to top radius (defined in the inset) with h/w.

created by applying uniaxial compression on the graphene sheets supported by SiO_2 substrate. Here we use the AIREBO potential[27] to account for carbon−carbon interactions and the 6−12 Lennard-Jones potential for nonbonding van der Waals interactions. The nonbonding O−C and Si−C interactions are described by the 6−12 L-J potential,[28] and the parameters are obtained by a combination rule with σ_{O-C} = 3.2185 Å, ε_{O-C} = 0.003 527 eV and σ_{Si-C} = 3.6035 Å, ε_{Si-C} = 0.005 668 eV. After stable structure is achieved by the empirical force field, we choose a part of the relaxed wrinkled graphene as the unit cell in which the width is 0.423 nm. The unit cell length is chosen to ensure that the distance between neighbored wrinkles is larger than 4.5 nm and avoid any self-interaction in neighbored wrinkles. In the periodic supercell, there is a vacuum region larger than 3 nm in the direction perpendicular to the wrinkle top. Similar periodic wrinkle structure has been successfully achieved in experiments.[19,25] Then the structural and electronic properties of the wrinkled graphene sheets are extensively studied by density function theory (DFT) calculations. All computations are performed in the VASP code by using the projector augmented wave method with the Perdew−Burke−Ernzerhof exchange-correlation functional.[29−31] First, the wrinkled graphene unit cell is relaxed by using a conjugate-gradient algorithm until the force on each atom is less than 0.1 eV/nm. Then an energy cutoff of 400 eV and special k points sampled on a 8 × 8 × 1 Monkhorst−Pack mesh[32] are employed to calculate exact electronic structure. The external electric field is modeled by adding a sawtooth-like potential along the perpendicular direction of the wrinkled graphene.[33]

3. RESULTS AND DISCUSSION

The geometry of graphene wrinkles is dependent on applied compression. The wrinkle height increases but the width decreases with increasing the compressive strain. To characterize the structure of the wrinkled graphene relaxed by the DFT technique, Figure 1b shows the variation of the size ratio h/w of wrinkle height to width under different compressive strain. The ratio h/w increases linearly with the compressive strain ε but increases sharply after ε is larger than 18%. This is due to the bottom parts of the wrinkles binding together, as shown in the inset of Figure 1b. With further increasing the height, the wrinkle will collapse onto the graphene sheet because of van der Waals interactions. Moreover, the curvature radius r of the wrinkle top decreases with increasing the ratio h/w. Figure 1c presents the variation of the ratio h/r of wrinkle height to top radius with h/w. The wrinkles are a kind of protrusion on the graphene sheets. The onset of field emission is related closely to the field enhancement factor and the work function. According to previous studies for a nanoprotrusion on a flat planar surface,[34,35] the field enhancement factor β of the wrinkle will approximately equal or be proportion to the size ratio h/r, namely $\beta \approx h/r$. The increase in h/r with enlarging wrinkle height leads to a larger field enhancement factor, which indicates a better field emission capability.

A free-standing single-layer graphene whose π orbitals intersect at the Dirac point has a zero band gap. According to the band structure in the inset of Figure 2, the wrinkled

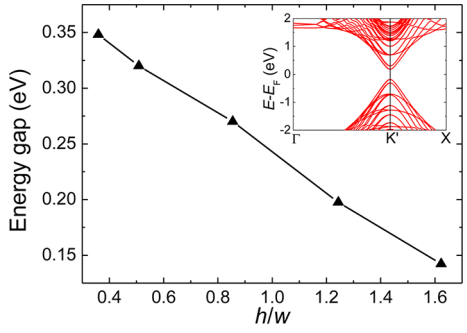

Figure 2. Energy gap of the wrinkled graphene with the size ratio h/w. The inset shows the band structure of a wrinkled graphene with h/w = 0.36.

graphene exhibits semiconducting properties. For the wrinkled graphene with h/w = 0.36, its energy gap is 0.36 eV. However, the energy gap monotonically decreases with the wrinkle size ratio h/w increases, as shown by Figure 2. The energy gap decreases to 0.14 eV when the ratio h/w is 1.62, and the corresponding change compared to the energy gap of h/w = 0.36 is over 60%. This means a strong influence from the wrinkle on the graphene band structure, and the electronic properties of wrinkled graphene can be effectively tuned by modifying the wrinkle morphology. The energy gap between the HOMO and the LUMO is considered to be closely related with chemical reactivity and field emission properties. A small energy gap suggests that it is energetically favorable to add electrons to a high-lying LUMO or to extract electrons from a low-lying HOMO.

dx.doi.org/10.1021/jp3103063 | J. Phys. Chem. C 2013, 117, 692−696

The work function (WF), ionization potential (IP), and electron affinity (EA) are critical parameters for studying and understanding the field emission properties of carbon nanomaterials. We have calculated the WFs, IPs, and EAs of the wrinkled-graphene sheets, which are shown in Figure 3. Here

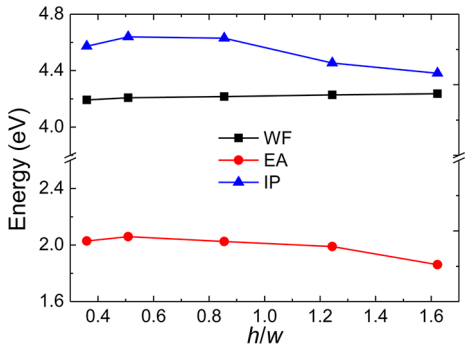

Figure 3. Work functions (WFs), electron affinities (EAs), and ionization potentials (IPs) of wrinkled graphene with h/w.

the work function of a wrinkled graphene is defined as the energy needed to take an electron from the Fermi level to the vacuum level. The WF of a flat graphene from our DFT calculation is 4.4 eV. Under compression, the calculated WF of the wrinkled graphene of h/w = 0.36 decreases to 4.2 eV. However, further change in the wrinkle size and geometry slightly influences the value of the WF, as shown in Figure 3. The WF of graphene sheet becomes insensitive to wrinkle after structural buckling. Theoretically, the IP and EA are defined as the energy differences between the cationic (with one positive charge) and anionic (with one negative charge) wrinkled graphene and the neutral one, respectively. For the wrinkled graphene of h/w = 0.36, its IP is 4.57 eV and EA is 2.0 eV. With the change of wrinkle height and width under a larger compression, the IP and EA for the wrinkled-graphene of h/w = 1.62 decrease to 4.38 and 1.86 eV, respectively. The field emission is qualitatively dependent on the IP and EA: the lower IP and EA, the easier for an electron to be emitted from the emitter and the higher field-emission current or the lower threshold voltage.[36,37] Therefore, the field emission performance of wrinkled graphene can be enhanced by introducing stronger structural deformation on the wrinkled part.

We now examine the charge density difference $\Delta\rho = \rho^{charged} - \rho$, where $\rho^{charged}$ and ρ are the charge densities of the charged and uncharged wrinkled graphene, respectively. The results in Figure 4a,c show that for both negatively and positively charged system the charge accumulation and depletion mostly distribute at the wrinkle top. It indicates that the electrons will be mainly emitted from the wrinkle top when the wrinkled graphene is used as field emitter. For the charged wrinkled graphene of h/w = 1.62 (Figure 4b,d), the charge accumulation and depletion become more concentrated at the top because of the increase in the curvature of wrinkle top, but the overall distribution pattern remains essentially unchanged. These observations explain the mechanism of the decrease in IP and EA as shown in Figure 3 and also suggest an enhanced field emission at highly wrinkled graphene. Naturally, the electron redistribution in the charged wrinkled graphene unveils a possible mechanism for the improved electron emission caused by structural protrusion in experiment.[14]

In field emission, electrons from a solid can be emitted into the vacuum only when overcoming an energy barrier at the

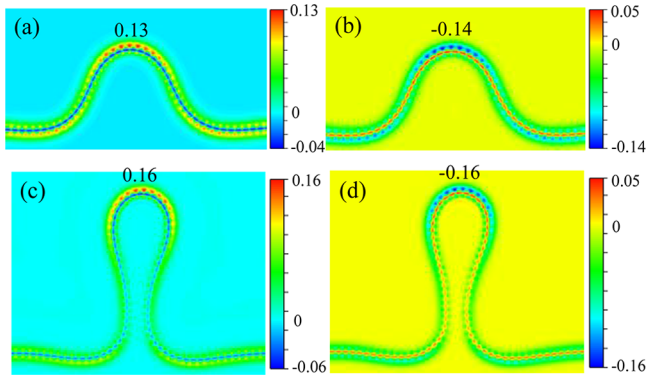

Figure 4. Contour plots of 2D projection of charge density changes [in units of e/Å^3] for the wrinkled graphene of h/w = 0.36 and 1.62 with injecting one negative charge (a) and (c) and one positive charge (b) and (d). The value and location of the largest charge density difference are shown in each panel.

solid−vacuum interface. To apply an external electric field is an effective way to reduce the energy barrier, which is identical to the WF of the solid. Figure 5 shows the variations of the WFs

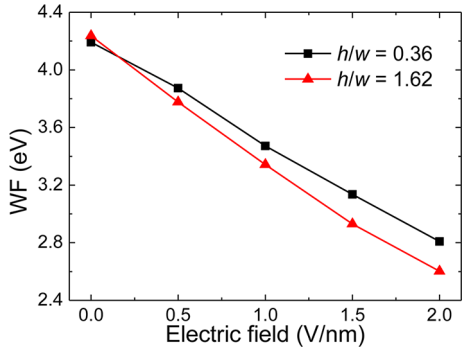

Figure 5. Work functions of the wrinkled graphene of h/w = 0.36 and 1.62 with bias.

of two wrinkled-graphene sheets under vertical electric fields. The WFs monotonically decrease with increasing the field, but the slope of the WF for the graphene of h/w = 1.62 is larger than that of h/w = 0.36. Under a bias of 2 V/nm, the WFs for graphene of h/w = 0.36 and 1.62 are 2.81 and 2.6 eV, respectively. This also means a better field emission for highly wrinkled graphene.

To further understand the field emission properties of wrinkled graphene, we have investigated the changes of the charge densities of the HOMO and LUMO and the local density of states (LDOS) in the presence of an electric field. The charge distributions of the HOMO and LUMO of the wrinkled graphene of h/w = 0.36 are shown in Figure 6a. The charges uniformly distribute at the wrinkled and flat parts of the graphene sheet in the absence of a field. Applying a bias of 1 V/nm, the HOMO of the wrinkled graphene almost disappears at the wrinkle top as shown by Figure 6b. On the contrary, the charge accumulation of the LUMO concentrates at the wrinkle top. The dramatic difference between the HOMO and LUMO at the wrinkled part under electric field demonstrates that the graphene wrinkles could be ideal electron emitting source. Furthermore, Figure 7a shows the LDOS of two atoms ($a1$ and $a2$) locating at the flat part of the graphene sheet and top part of the wrinkle. The positions of $a1$ and $a2$ are denoted by the

dx.doi.org/10.1021/jp3103063 | J. Phys. Chem. C 2013, 117, 692−696

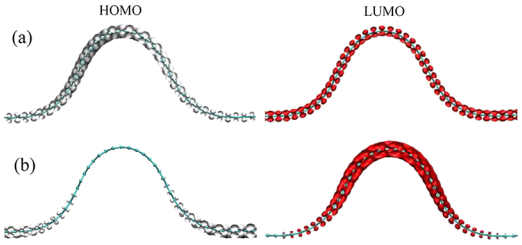

Figure 6. Isosurfaces of the charge densities of the HOMO and LUMO [in unit of 0.005 e/Å^3] for the wrinkle of h/w = 0.36 in the absence (a) and presence (b) of a bias of 1 V/nm.

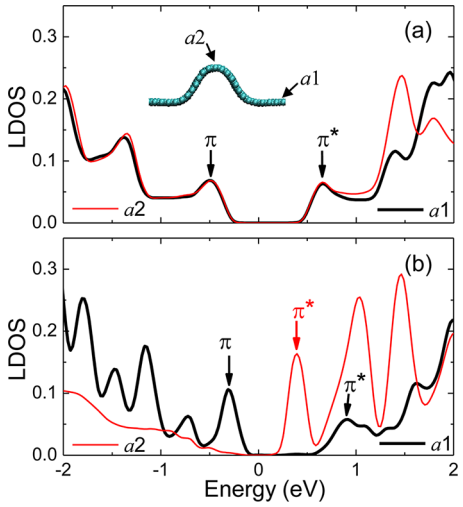

Figure 7. (a) LDOS (in units of states/atom) of the *a*1 and *a*2 atoms denoted by the inset for the wrinkled graphene of h/w = 0.36. (b) LDOS of the *a*1 and *a*2 atoms under a bias of 1 V/nm.

inset of Figure 7a. Without electric field, the distribution of the LDOS and the π and π^* states for the two atoms are approximately the same around the Fermi level, indicating slight influence from the structural deformation. However, the π and π^* states of the *a*2 atom are significantly changed and modified when a bias of 1 V/nm is applied, as shown in Figure 7b. The LDOS of the *a*1 atom below the Fermi level is higher than that of the *a*2 atom, while it is lower above the Fermi level. So the wrinkled and flat parts of the graphene sheet possess quite different electronic properties under an external electric field. This modification is mainly due to the charge localization and concentration at the wrinkle (Figure 6).

With increasing structural size and external perturbation, the graphene wrinkle will collapse and transform into folded wrinkle. Here the field emission properties of such folded graphene wrinkle have been studied by the same DFT technique, as shown in Figure 8. The height and width of this folded wrinkle are 1.20 and 5.33 nm, respectively. The WF of the folded-wrinkle graphene is 4.257 eV, slightly larger than that of the wrinkled graphene presented in Figure 3. The charge density changes for the folded-wrinkle graphene when injecting one negative and one positive charge are shown in Figure 8. The charge accumulation and depletion mostly distribute at the left and right top curved parts of the folded wrinkle. Because of stronger structural deformation, the IP and EA of the folded wrinkle decrease to 3.72 and 1.67 eV, respectively. In the presence of a bias of 1 V/nm, its work function decreases to 3.368 eV. All those results suggest that the folded wrinkle also could be a good candidate for field emitter.

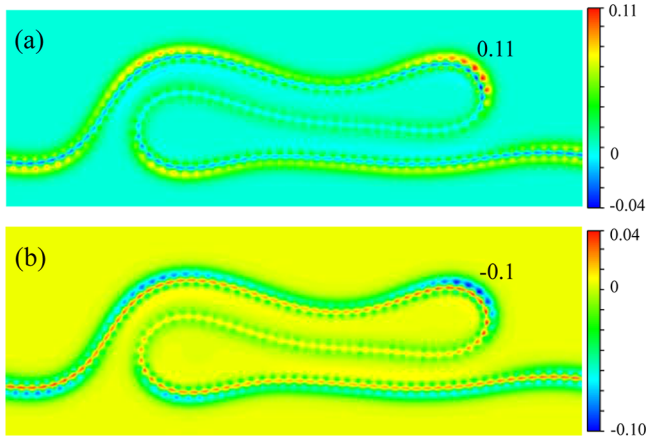

Figure 8. Contour plots of 2D projection of charge density changes [in units of e/Å^3] for the graphene with folded wrinkle when injecting (a) one negative charge and (b) one positive charge. The value and location of the largest charge density difference are shown in each panel.

4. CONCLUSIONS

Our first-principles calculations reveal sensitive response of the electronic properties of wrinkled graphene to charge injecting and external electric field. The field enhancement factor of the wrinkled graphene increases, but electron affinities and ionization potentials decrease with increasing the curvature of wrinkle top. When injecting charges, both the charge accumulation and depletion mostly locate at the wrinkle top parts and become more concentrated in the wrinkle with a higher curvature. Under a bias, the change of the HOMO and LUMO mainly appears at the wrinkled parts, especially at its top. It is indicated that the electrons are easily emitted from the graphene wrinkles. The present results shed lights on the fundamental behaviors of wrinkled graphene, which can be explored for innovative application in field emission.

AUTHOR INFORMATION

Corresponding Author

*E-mail yfguo@nuaa.edu.cn (Y. Guo), wlguo@nuaa.edu.cn (W. Guo); Ph 86-25-84890513; Fax 86-25-84895827.

Notes

The authors declare no competing financial interest.

ACKNOWLEDGMENTS

This work is supported by the 973 Program (2013CB932604, 2012CB933403), the NSF (11072109, 91023026), and the Fundamental Research Funds for the Central Universities (No. NE2012005) of China.

REFERENCES

(1) Bunch, J. S.; van der Zande, A. M.; Verbridge, S. S.; Frank, I. W.; Tanenbaum, D. M.; Tanenbaum, D. M.; Parpia, J. M.; Craighead, H. G.; McEuen, P. L. *Science* **2007**, *315*, 490−493.

(2) Lee, C.; Wei, X. D.; Kysar, J. W.; Hone, J. *Science* **2008**, *321*, 385−388.

(3) Meyer, J. C.; Geim, A. K.; Katsnelson, M. I.; Novoselov, K. S.; Booth, T. J.; Roth, S. *Nature* **2007**, *446*, 60−63.

(4) Novoselov, K. S.; Geim, A. K.; Morozov, S. V.; Jiang, D.; Katsnelson, M. I.; Grigorieva, I. V.; Dubonos, S. V.; Firsov, A. A. *Nature* **2005**, *438*, 197−200.

(5) Geim, A. K.; Novoselov, K. S. *Nat. Mater.* **2007**, *6*, 183−191.

(6) Miao, F.; Wijeratne, S.; Zhang, Y.; Coskun, U. C.; Bao, W.; Lau, C. N. *Science* **2007**, *317*, 1530−1533.
(7) Wu, Z. S.; Pei, S.; Ren, W.; Tang, D.; Gao, L.; Liu, B.; Li, F.; Liu, C.; Cheng, H. M. *Adv. Mater.* **2009**, *21*, 1756−1760.
(8) Eda, G.; Unalan, H. E.; Rupesinghe, N.; Amaratunga, G. A. J.; Chhowalla, M. *Appl. Phys. Lett.* **2008**, *93*, 233502 1−3.
(9) Uppireddi, K.; Rao, C. V.; Ishikawa, Y.; Weiner, B. R.; Morell, G. *Appl. Phys. Lett.* **2010**, *97*, 062106 1−3.
(10) Baby, T. T.; Ramaprabhua, S. *Appl. Phys. Lett.* **2011**, *98*, 183111 1−3.
(11) Yamaguchi, H.; Murakami, K.; Eda, G.; Fujita, T.; Guan, P.; Wang, W.; Gong, C.; Boisse, J.; Miller, S.; Acik, M. M.; et al. *ACS Nano* **2011**, *5*, 4945−4952.
(12) Xiao, Z. M.; She, J. C.; Deng, S. Z.; Tang, Z. K.; Li, Z. B.; Lu, J. M.; Xu, N. S. *ACS Nano* **2010**, *4*, 6332−6336.
(13) Wei, X. L.; Bando, Y.; Golberg, D. *ACS Nano* **2012**, *6*, 705−711.
(14) Ye, D.; Moussa, S.; Ferguson, J. D.; Baski, A. A.; El-Shall, M. S. *Nano Lett.* **2012**, *12*, 1265−1268.
(15) Xu, K.; Cao, P. G.; Heath, J. R. *Nano Lett.* **2009**, *9*, 4446−4451.
(16) Li, X.; Cai, W.; An, J.; Kim, S.; Nah, J.; Yang, D.; Piner, R.; Velamakanni, A.; Jung, I.; Tutuc, E.; et al. *Science* **2009**, *324*, 1312−1314.
(17) Sun, G. F.; Jia, J. F.; Xue, Q. K.; Li, L. *Nanotechnology* **2009**, *20*, 355701 1−4.
(18) Prakash, G.; Capano, M. A.; Bolen, M. L.; Zemlyanov, D.; Reifenberger, R. G. *Carbon* **2010**, *48*, 2383−2393.
(19) Pan, Z.; Liu, N.; Fu, L.; Liu, Z. *J. Am. Chem. Soc.* **2011**, *133*, 17578−17581.
(20) Barboza, A. P. M; Chacham, H.; Oliveira, C. K.; Fernandes, T. F. D.; Ferreira, E. H. M.; Archanjo, B. S.; Batista, R. J. C.; de Oliveira, A. B.; Neves, B. R. A. *Nano Lett.* **2012**, *12*, 2313−2317.
(21) Bao, W.; Miao, F.; Chen, Z.; Zhang, H.; Jang, W.; Dames, C.; Lau, C. N. *Nat. Nanotechnol.* **2009**, *4*, 562−566.
(22) Li, Z. J.; Cheng, Z. G.; Wang, R.; Li, Q.; Fang, Y. *Nano Lett.* **2009**, *9*, 3599−3602.
(23) Kim, K.; Lee, Z.; Malone, B. D.; Chan, K. T.; Alemán, B.; Regan, W.; Gannett, W.; Crommie, M. F.; Cohen, M. L.; Zettl, A. *Phys. Rev. B* **2011**, *83*, 245433 1−8.
(24) Zhu, W.; Low, T.; Perebeinos, V.; Bol, A. A.; Zhu, Y.; Yan, H.; Tersoff, J.; Avouris, P. *Nano Lett.* **2012**, *12*, 3431−3436.
(25) Wang, Y.; Yang, R.; Shi, Z.; Zhang, L.; Shi, D.; Wang, E.; Zhang, G. *ACS Nano* **2011**, *5*, 3645−3650.
(26) Plimpton, S. *J. Comput. Phys.* **1995**, *117*, 1−19.
(27) Brenner, D. W.; Shenderova, O. A.; Harrison, J. A.; Stuart, S. J.; Ni, B.; Sinnott, S. B. *J. Phys.: Condens. Matter* **2002**, *14*, 783−802.
(28) Cornell, W. D.; Cieplak, P.; Bayly, C. I.; Gould, I. R.; Merz, K. M., Jr.; Ferguson, D. M.; Spellmeyer, D. C.; Fox, T.; Caldwell, J. W.; Kollman, P. A. *J. Am. Chem. Soc.* **1995**, *117*, 5179−5197.
(29) Blochl, P. E. *Phys. Rev. B* **1994**, *50*, 17953−17979.
(30) Kresse, G.; Joubert, D. *Phys. Rev. B* **1999**, *59*, 1758−1775.
(31) Perdew, J. P.; Burke, K.; Ernzerhof, M. *Phys. Rev. Lett.* **1996**, *77*, 3865−3868.
(32) Monkhorst, H. J.; Pack, J. D. *Phys. Rev. B* **1976**, *13*, 5188−5192.
(33) Neugebauer, J.; Scheffler, M. *Phys. Rev. B* **1992**, *46*, 16067−16080.
(34) Bonard, J. M.; Dean, K. A.; Coll, B. F.; Klinke, C. *Phys. Rev. Lett.* **2002**, *89*, 197602 1−4.
(35) Forbes, R. G.; Edgcombe, C. J.; Valdre, U. *Ultramicroscopy* **2003**, *95*, 57−65.
(36) An, W.; Wu, X. J.; Zeng, X. C. *J. Phys. Chem. B* **2006**, *110*, 16346−16352.
(37) Qiao, L.; Zheng, W. T.; Xu, H.; Zhang, L.; Jiang, Q. *J. Chem. Phys.* **2007**, *126*, 164702 1−7.